Syntheses and Single-Crystal X-ray Structures of a Series of Monosubstituted cis , cis -1,3,5-Triaminocyclohexane-Based Complexes

ARTICLE *in* INORGANIC CHEMISTRY · JUNE 1997

Impact Factor: 4.76 · DOI: 10.1021/ic9614529

Syntheses and Single-Crystal X-ray Structures of a Series of Monosubstituted *cis,cis*-1,3,5-Triaminocyclohexane-Based Complexes

Leroy Cronin,[†] Bryan Greener,[†] Simon P. Foxon,[†] Sarah L. Heath,[‡,§] and Paul H. Walton*[,†]

Department of Chemistry, University of York, Heslington, York, YO1 5DD, U.K., and Department of Chemistry, University of Newcastle-upon-Tyne, Newcastle, NE1 7RY, U.K.

Received December 4, 1996[⊗]

The four triimine compounds *cis,cis*-1,3,5-tris[(*E*)-(X)-benzylideneamino]cyclohexane [X = H (**1**); 3-hydroxy (**2**); 3,5-dimethoxy (**3**); 4-acetamido (**4**)] are synthesized by the condensation of *cis,cis*-1,3,5-triaminocyclohexane with a substituted aromatic aldehyde. Complexation of these ligands with metal salts (**1** with Ni, Cu, and Zn salts; **2** and **3** with Cu salts; **4** with a Zn salt) causes a selective hydrolysis reaction producing new monoimine complexes. The resulting complexes are characterized by a combination of infrared spectroscopy, elemental analysis, mass spectrometry and, in the cases of the zinc complexes, ^{1}H NMR spectroscopy. The structures of all six complexes are confirmed by single-crystal X-ray crystallographic studies.

Introduction

The molecule *cis,cis*-1,3,5-triaminocyclohexane (tach) has been known for several years as a versatile face-capping N_3 ligand. It can form complexes with a large number of the first-row transition metals[1−4] and can be easily derivatized to give hexadentate ligands.[5−7] More recently, tach has attracted the attention of bioinorganic chemists, where it has been used in the synthesis of *in vivo* metal chelators[8,9] and in the modeling of metalloenzyme active sites.[10−12] For example, studies on tach have shown that its complex with zinc(II), $Zn(tach)^{2+}$, is a particularly effective mimic of the active site of carbonic anhydrase.[10,11] This is because a water molecule bound to $Zn(tach)^{2+}$ has a pK_a of 7.95, similar to that of the analogous water molecule in carbonic anhydrase (∼7). Furthermore, the amine groups on tach can be easily and systematically derivatized to afford a wide range of possible ligands. For instance, we have recently[12] prepared derivatized tach complexes to model the primary and secondary coordination environment of the zinc ion found in carbonic anhydrase. As such, tach offers considerable potential as a basis for new ligands in bioinorganic modeling chemistry.

In this paper we describe the synthesis and structural characterization of new monosubstituted tach-based complexes. The synthesis is quite general and can be carried out with a range of metal salts and ligands in good yield.[12,13] The resulting complexes demonstrate rigid "superstructures" that can be systematically varied. Notably, similar monosubstituted face-capping ligands have proved demanding to synthesize in the past.[14−16]

Experimental Section

Materials and Methods. All reagents with the exception of phloroglucinol (Lancaster Chemicals Ltd.) were purchased from the Aldrich Chemical Co. and used without further purification. *cis,cis*-1,3,5-Triaminocyclohexane (tach) was synthesized according to literature methods.[5] Solvents for synthesis (AR grade) were supplied by Fisons Ltd. and were also used without further purification. Deuterated solvents were obtained from Goss Scientific. Melting points were determined using an Electrothermal 1100 microprocessor controlled apparatus. Densities were measured by flotation of crystals in a mixed solvent system, bromoform/hexane. FT ^{1}H NMR were acquired on a JEOL EX270 spectrometer, and spectra were referenced using the signal from the residual solvent protons. Infrared spectra were acquired using KBr pressed pellets (pressed under 7.0 tonnes pressure) on a Mattson Sirius Research Series FTIR spectrometer. Mass spectra were acquired on a Fisons Instruments Autospec using a 0−650 °C temperature range. Crystallographic data were collected with a MSC Rigaku AFC6S (**5**−**9**) diffractometer and a Siemens SMART CCD diffractometer (**10**). Elemental analyses were performed by Butterworth Laboratories Ltd., 54−56 Waldegrave Road, Teddington, Middlesex, England.

Ligand Synthesis. (a) *cis,cis*-1,3,5-Tris[(*E*)-benzylideneamino]-cyclohexane (1). Tach·3HCl (0.50 g, 2.10 mmol) and sodium hydroxide (0.25 g, 6.30 mmol) were dissolved in water (3.2 cm^3). This was stirred vigorously with a solution of benzaldehyde (0.67 g, 6.30 mmol) in diethyl ether (4.2 cm^3) for 6 h. The ether layer was removed and the aqueous phase extracted with ether (3 cm^3). The ether phases were combined and had an equal volume of hexane added. Crystals precipitated overnight. The supernatant solution was decanted and left to precipitate further crystals. The combined crystals were washed with hexane (2 × 10 cm^3) and dried in air at room temperature (0.50 g, 1.27 mmol, 60%). mp: 80.0−80.5 °C (lit.[17] mp 87−89 °C). ^{1}H NMR

[†] University of York.
[‡] University of Newcastle-upon-Tyne.
[§] Present address: Department of Chemistry, University of Sheffield, Brook Hill, Sheffield, S3 7HF, U.K.
[⊗] Abstract published in *Advance ACS Abstracts,* May 15, 1997.

(1) Wentworth, R. A. D.; Felten, J. J. *J. Am. Chem. Soc.* **1968**, *90*, 621.
(2) Wentworth, R. A. D. *Inorg. Chem.* **1968**, *7*, 1030.
(3) Urbach, F. L.; Sarneski, J. E.; Turner, L. J.; Busch, D. H. *Inorg. Chem.* **1968**, *7*, 2169.
(4) Sarneski, J. E.; McPhail, A. T.; Onan, K. D. *J. Am. Chem. Soc.* **1977**, *99*, 7376.
(5) Lions, F.; Martin, K. V. *J. Am. Chem. Soc.* **1957**, *79*, 1572.
(6) Gillum, W. O.; Wentworth, R. A. D.; Childers, R. F. *Inorg. Chem.* **1970**, *9*, 1825.
(7) Wentworth, R. A. D. *Inorg. Chem.* **1971**, *10*, 2615.
(8) Bollinger, J. E.; Mague, J. T.; Banks,W. A.; Kastin A. J.; Roundhill D. M. *Inorg. Chem.* **1995**, *34*, 2143.
(9) Bollinger, J. E.; Mague, J. T.; O'Connor, C. J.; Banks,W. A.; Roundhill, D. M. *J. Chem. Soc., Dalton Trans.* **1995**, 1677.
(10) Fujii, Y.; Itoh, T.; Onodera, K.; Tada, T. *Chem. Lett.* **1995**, 307.
(11) Itoh, T.; Fujii, Y.; Tada, T.; Yoshikawa, Y.; Hisada, H. *Bull. Chem. Soc. Jpn.* **1996**, *69*, 1265.
(12) Greener, B.; Moore, M. H.; Walton, P. H. *Chem. Commun.* **1996,** 27.
(13) Greener, B.; Cronin, L.; Wilson, G. D.; Walton, P. H. *J. Chem. Soc., Dalton Trans.* **1996**, 401.
(14) Kimura, E.; Nakamura, I.; Koike, T.; Shionoya, M.; Kodama, Y.; Ikeda, T.; Shiro, M. *J. Am. Chem. Soc.* **1994**, *116*, 4764.
(15) Meunier, I.; Mishra, A. K.; Hanquet, B.; Cocolios, P.; Guilard, R. *Can. J. Chem.* **1995**, *73*, 685.
(16) Farrugia, L. J.; Lovatt, P. A.; Peakcock, R. D. *Inorg. Chim. Acta* **1996**, *246*, 343.
(17) Stetter, H.; Bremen, *J. Chem. Ber.* **1973**, *106*, 2523.

S0020-1669(96)01452-8 CCC: $14.00

($CDCl_3$, 270 MHz): δ 8.38 (s, 3H, C*H*═N), 7.74 (m, 6H, Ar*H*), 7.41 (m, 9H, Ar*H*), 3.59 [tt, 3H, $^3J_{HH}$ = 3 Hz, $^3J_{HH}$ = 12 Hz, >C*H*(N═CH)], 2.04 [dt, 3H, $^3J_{HH}$ = 12 Hz, $^2J_{HH}$ = 12 Hz, >C*H*(H)], 1.00 [dt, 3H, $^2J_{HH}$ = 12 Hz, $^3J_{HH}$ = 3 Hz, C*H*(H)]. IR cm^{-1} (KBr pressed pellet): 2900 (s), 2800 (s), 1650 (s), 750 (s), 690 (s). MS CI: +ve ion *m/z* = 394 (MH^+).

(b) *cis,cis*-1,3,5-Tris[(*E*)-(3-hydroxybenzylidene)amino]cyclohexane (2). Tach·3HCl (0.25 g, 1.05 mmol) and sodium hydroxide (0.126 g, 3.15 mmol) were dissolved in water (2 cm^3)/methanol (10 cm^3). A solution of 3-hydroxybenzaldehyde (0.385 g, 3.15 mmol) in methanol (50 cm^3) was added and the whole solution refluxed for 1 h. The resulting pale yellow solution was reduced *in vacuo* until precipitation began to occur and then left to stand at 5 °C overnight. A white solid formed, which was filtered off and washed with methanol. The residue was dried under vacuum at room temperature, producing the product as a white powder (0.37 g, 0.84 mmol, 80%). mp: 161−162 °C. ^{1}H NMR (CD_3OD, 270 MHz): δ 8.43 (s, 3H, C*H*═N), 7.27 (m, 10H, Ar*H*), 6.93 (m, 2H, Ar*H*), 4.95 (s, H_2O), 3.67 [tt, 3H, $^3J_{HH}$ = 12 Hz, $^3J_{HH}$ = 4 Hz, >C*H*(N═CH)], 2.04 [dt, 3H, $^2J_{HH}$ = 12 Hz, $^3J_{HH}$ = 12 Hz, >C*H*(H)], 1.90 [dt, 3H, $^2J_{HH}$ = 12 Hz, $^3J_{HH}$ = 4 Hz, >C*H*(H)]. IR cm^{-1} (KBr pressed pellet): 3500−3000 (s), 2940 (s), 2861 (s), 1644 (s), 1596 (s), 1453 (s), 1349 (m), 1291 (s), 1248 (s), 1174 (m), 1155 (m), 864 (m), 783 (s), 685 (s). MS LRFAB(NOBA matrix) +ve ion *m/z* = 442 (MH^+). Anal. Calcd for $C_{27}H_{27}N_3O_3 \cdot H_2O$ actual (expected): C, 70.19 (70.57); H, 6.52 (6.36); N, 8.88 (9.15).

(c) *cis,cis*-1,3,5-Tris[(*E*)-(3,5-dimethoxybenzylidene)amino]cyclohexane (3). Tach·3HCl (1.00 g, 4.19 mmol) and sodium hydroxide (0.50 g, 12.6 mmol) were dissolved in water (2 cm^3)/methanol (25 cm^3). To this, a solution of 3,5-dimethoxybenzaldehyde (2.09 g, 12.6 mmol) in methanol (25 cm^3) was added and the whole solution stirred at ambient temperature. After 3.5 h, a white precipitate had formed, which was filtered off and the residue washed with methanol. Drying the residue under vacuum for 1 h gave the product as a white powder (1.86 g, 3.24 mmol, 78%). mp: 150−150.5 °C. ^{1}H NMR (CD_3OD, 270 MHz): δ 8.43 (s, 3H, C*H*═N), 7.00 (d, 6H, $^4J_{HH}$ = 2 Hz, ArH_o), 6.62 (t, 3H, $^4J_{HH}$ = 2 Hz, ArH_p), 3.85 (s, 18H, OCH_3), 3.69 [tt, 3H, $^3J_{HH}$ = 12 Hz, $^3J_{HH}$ = 4 Hz, >C*H*(N═CH)], 2.05 [dt, 3H, $^2J_{HH}$ = 12 Hz, $^3J_{HH}$ = 12 Hz, >C*H*(H)], 1.91 [dt, 3H, $^2J_{HH}$ = 12 Hz, $^3J_{HH}$ = 4 Hz, >C*H*(H)]. IR cm^{-1} (KBr pressed pellet): 3625−3325 (s), 1640 (m), 1593 (s), 1461 (s), 1428 (m), 1353 (m), 1300 (m), 1206 (s), 1158 (s), 1065 (m). MS LRFAB(NOBA matrix) +ve ion *m/z* = 574 (MH^+). Anal. Calcd for $C_{33}H_{39}O_6N_3$, actual (expected): C, 69.24 (69.09); H, 6.48 (6.85); N, 7.18 (7.33).

(d) *cis,cis*-1,3,5-Tris[(*E*)-(4-acetamidobenzylidene)amino]cyclohexane (4). Tach·3HCl (0.50 g, 2.10 mmol) and sodium hydroxide (0.25 g, 6.30 mmol) were dissolved in water (2 cm^3)/methanol (15 cm^3). To this, a solution of 4-acetamidobenzaldehyde (1.03 g, 6.30 mmol) in methanol (20 cm^3) was added and left to reflux for 3 h. Reducing the cooled solution *in vacuo* gave a solid which was then dispersed in water (50 cm^3) and sonicated for 30 min. Filtering the dispersion produced the product as a yellow powder (0.73 g, 1.29 mmol, 62%). mp: 167−168 °C. ^{1}H NMR (CD_3OD, 270 MHz): δ 8.43 (s, 3H, C*H*═N), 7.72 (m, 12H, Ar*H*), 4.95 (s, H_2O), 3.65 (tt, 3H, $^3J_{HH}$ = 12 Hz, $^3J_{HH}$ = 4 Hz, >C*H*(N═CH), 2.17 (s, 9H, CH_3), 2.03 [dt, 3H, $^2J_{HH}$ = 12 Hz, $^3J_{HH}$ = 12 Hz, >C*H*(H)], 1.92 [dt, 3H, $^2J_{HH}$ = 12 Hz, $^3J_{HH}$ = 4 Hz, >C*H*(H)]. IR cm^{-1} (KBr pressed pellet): 3248 (s), 3183 (s), 3106 (s), 3041 (s), 2930 (s), 2856 (s), 1676 (s), 1639 (s), 1595 (s), 1535 (s), 1513 (s), 1412 (m), 1371 (m), 1317 (s), 1264 (s), 1221 (m), 1173 (s), 1018 (m), 838 (m). MS LRFAB(NOBA matrix) +ve ion *m/z* = 565 (MH^+). Anal. Calcd for $C_{33}H_{36}N_6O_3 \cdot 2^1/_2H_2O$, actual (expected): C, 64.71 (65.00); H, 6.85 (6.78); N, 14.29 (13.79).

Complex Synthesis. (a) *r*-1-[(*Z*)-Benzylideneamino-κN]-*c*-3,*c*-5-diamino-κ^2N,N'-cyclohexanebis(nitrato-κO)nickel(II) (5). Nickel(II) nitrate hexahydrate (0.37 g, 1.3 mmol) was dissolved in methanol (5 cm^3). This was added to a stirred solution of **1** (0.51g, 1.3 mmol) in methanol (5 cm^3). Within seconds a pale blue precipitate had formed; this was filtered off and washed with methanol (5 cm^3). The solution preciptated further batches of product which were isolated in the same way. The combined products were dried *in vacuo* at room temperature giving the product as pale blue crystals (0.40 g, 1.0 mmol, 77%). mp: 280−281 °C (dec). IR cm^{-1} (KBr pressed pellet): 3314 (s), 3294 (s), 3263 (s), 3176 (s), 2906 (s), 1619 (s), 1596 (s), 1478 (s), 1454 (s), 1441 (s), 1421 (s), 1404 (m), 1385 (m), 1367 (m), 1307 (s), 1285 (s), 692 (m). MS LRFAB(NOBA matrix) +ve ion *m/z* = 337 ($M^+ - NO_3^-$). Anal. Calcd for $C_{13}H_{19}N_5O_6Ni$, actual (expected): C, 39.10 (39.03); H, 4.58 (4.79); N, 17.64 (17.51). Measured density: 1.59(5) g cm^{-3}.

(b) *r*-1-[(*Z*)-Benzylideneamino-κN]-*c*-3,*c*-5-diamino-κ^2N,N'-cyclohexane bis(acetato-κO)copper(II) (6). Copper(II) acetate dihydrate (0.09 g, 0.45 mmol) was dissolved in methanol (~8 cm^3) with stirring and minimum heating. To this a solution of **1** (0.20 g, 0.51 mmol) in methanol (5 cm^3) was added dropwise. On standing for 48 h, the resulting blue solution precipitated the product as blue crystals (0.14 g, 0.35 mmol, 68%). mp: 235−235.5 °C (dec). IR cm^{-1} (KBr pressed pellet): 3233 (s), 3138 (m), 2935 (m), 2919 (s), 2891 (s), 1637 (s), 1615 (s), 1608 (s), 1600 (s), 1589 (s), 1580 (s), 1567 (s), 1463 (m), 1428 (m), 1400 (s), 1388 (s), 1360 (m), 1351 (m), 1338 (m), 1327 (s), 1306 (m), 1174 (s), 770 (s), 733 (m), 701 (m), 662 (m), 656 (m), 629 (m). MS LRFAB(NOBA matrix) +ve ion *m/z* = 280 (peak from ^{63}Cu) (M^+, $-2OAc^-$). Anal. Calcd for $C_{17}H_{25}N_3O_4Cu$, actual (expected): C, 51.39 (51.18); H, 6.20 (6.32); N, 10.60 (10.53). Measured density: 1.47(5) g cm^{-3}.

(c) *r*-1-[(*Z*)-Benzylideneamino-κN]-*c*-3,*c*-5-diamino-κ^2N,N'-cyclohexanechlorozinc(II) tetraphenylborate·CH_3OH (7). **1** (0.05 g, 0.13 mmol) was dissolved in methanol (5 cm^3). To this, a solution of zinc(II) chloride (0.02 g, 0.13 mmol) and sodium tetraphenylborate (0.04 g, 0.13 mmol) in methanol (3 cm^3) was added dropwise. The resulting solution was left to stand overnight. Large, colorless crystals formed and were filtered off. Drying *in vacuo* gave the product as colorless crystals (0.06 g, 0.09 mmol, 69%). mp: 186.5−187 °C. ^{1}H NMR (CD_3OD, 270 MHz): δ 8.85 (s, 1H N═C*H*), 8.07 (d, 2H, ArH_o), 7.47 (m, 3H, Ar*H*), 4.34 (m, 1H, CR_2H), 3.74 (m, 2H, CR_2H), 2.24 (m, 6H, >CH_2); *tetraphenylborate resonances*, δ 7.38 (m, 8H, Ar*H*), 6.85 (m, 8H, Ar*H*), 6.71 (m, 4H, Ar*H*). IR cm^{-1} (KBr pressed pellet): 3284 (s), 3241 (s), 2999 (s), 1634 (s), 1580 (s), 1479 (m), 1447 (m), 1426 (m), 1141 (s), 747 (s), 736 (s), 709 (s), 690 (s). MS FAB +ve ion *m/z* = 316 ($M^+ - BPh_4^-$). Anal. Calcd for $C_{37}H_{39}N_3ZnClB \cdot CH_3OH$: actual (expected): C, 68.11 (68.18); H, 6.39 (6.47); N, 6.48 (6.28). Measured density: 1.29(5) g cm^{-3}.

(d) *r*-1-[(*Z*)-(3-Hydroxybenzylidene)amino-κN]-*c*-3,*c*-5-diamino-κ^2N,N'-cyclohexanebis(acetato-κO)copper(II) (8). Copper(II) acetate monohydrate (0.41 g, 2.00 mmol) was dissolved in methanol (~150 cm^3) with stirring and minimum heating. To this, a solution of **2** (0.90 g, 2.00 mmol) in methanol (50 cm^3) was added dropwise. The resulting green solution was reduced *in vacuo* to ~30 cm^3, at which point hexane (5 cm^3) was added dropwise to precipitate a blue solid. This was filtered off and washed with cold methanol. The solution was further reduced and then cooled to afford further blue solid, which was isolated by filtration. The combined residues were dried in air and then *in vacuo* at room temperature to produce the product as a deep blue powder, (0.50 g, 1.20 mmol, 60%). mp: 202−204 °C (dec). IR cm^{-1} (KBr pressed pellet): 3220 (s), 3136 (s), 1689 (m), 1626 (m), 1612 (m), 1577 (s), 1426 (m), 1397 (s), 1381 (s), 1327 (m), 1301 (m), 1176 (m), 923 (m), 857 (m), 693 (m), 665 (m). MS LRFAB(NOBA matrix) +ve ion *m/z* = 296 (peak from ^{63}Cu) (M^+, $-2CH_3CO_2^-$). Anal. Calcd for $C_{17}H_{25}N_3O_5Cu$, actual (expected): C, 49.55 (49.21); H, 5.93 (6.07); N, 10.01 (10.13). Measured density; 1.51 (5) g cm^{-3}.

(e) *r*-1-[(*Z*)-(3,5-dimethoxybenzylidene)amino-κN]-*c*-3,*c*-5-diamino-κ^2N,N'-cyclohexanedichlorocopper(II) (9). Copper chloride dihydrate (0.44 g, 2.60 mmol) was dissolved in methanol (~150 cm^3) with stirring and minimum heating. To this **3** (1.49 g, 2.60 mmol) was added. The mixture was then left for 0.5 h while the ligand dissolved to give a green solution, which was then reduced *in vacuo* to ~10 cm^3. Hexane (2 cm^3) was added dropwise followed by methanol (1 cm^3). Shaking caused the solution to precipitate a blue solid, which was filtered off and washed with cold methanol. The product was dried in air and then *in vacuo* at room temperature to produce the product as a blue powder (0.73 g, 1.77 mmol, 68%). mp: 160−165 °C (dec). IR cm^{-1} (KBr pressed pellet): 3258 (m), 3215 (m), 3144 (m), 1629 (m), 1596 (s), 1468 (m), 1455 (m), 1418 (m), 1338 (m), 1215 (m), 1159 (s), 1065 (s), 841 (m), 682 (m). MS LRFAB(NOBA matrix) +ve ion *m/z* = 375 (peak from ^{63}Cu) ($M^+ - Cl^-$), 340 ($M^+ - 2Cl^-$). Anal. Calcd for $C_{15}H_{23}N_3O_2Cl_2Cu \cdot {}^1/_2H_2O$, actual (expected): C, 42.74 (42.81); H, 5.54 (5.75); N, 9.80 (9.99). Measured density: 1.59(5) g cm^{-3}.

Table 1[a]

	5	**6**	**7**	**8**	**9**	**10**
formula	$C_{13}H_{19}N_5NiO_6$	$C_{17}H_{25}N_3CuO_4$	$C_{38}H_{43}BClN_3OZn$	$C_{17}H_{25}CuN_3O_5$	$C_{15}H_{23}Cl_2CuN_3O_2$	$C_{39.7}H_{46.8}BClN_4O_{2.70}Zn$
fw	400.05	398.95	669.38	414.95	411.80	734.84
crystal size, mm	0.4 × 0.3 × 0.2	0.4 × 0.3 × 0.2	0.7 × 0.7 × 0.4	0.5 × 0.3 × 0.2	0.3 × 0.2 × 0.2	0.2 × 0.1× 0.1
crystal system	monoclinic	orthorhombic	triclinic	orthorhombic	triclinic	monoclinic
space group	$P2_1/c$	$Cmc21$	$P\bar{1}$	$Pnma$	$P\bar{1}$	$C2/c$
a, Å	8.237(1)	10.275(2)	12.757(4)	20.183(11)	9.873(7)	42.978(5)
b, Å	10.065(1)	19.345(6)	13.025(9)	10.336(8)	11.348(5)	11.535(2)
c, Å	19.464(3)	9.025(4)	10.684(3)	8.737(3)	9.343(4)	16.482(2)
α, deg	90	90	97.57(3)	90	107.44(4)	90
β, deg	94.152(12)	90	102.43(3)	90	114.62(4)	97.644(3)
γ, deg	90	90	87.77(4)	90	73.35(4)	90
V, Å^3	1609.4(4)	1794.0(10)	1718.4(14)	1823(2)	891.9(8)	8064(2)
Z	4	4	2	4	2	8
density calc/meas, g cm^{-1}	1.65/1.59(5)	1.48/1.47(5)	1.29/1.29(5)	1.51/1.50(5)	1.53/1.59(5)	1.21/1.25(5)
μ, cm^{-1}	12.49	12.43	8.26	12.31	15.35	7.14
range of transm factors	0.85−1.00	0.70−1.00	0.70−1.00	0.80−1.00	0.80−1.00	
temp, K	293(2)	293(2)	298(2)	293(2)	293(2)	160(2)
scan type	$\omega/2\theta$	$\omega/2\theta$	$\omega/2\theta$	$\omega/2\theta$	$\omega/2\theta$	ω
scan/frame* width (deg)	0.95 + 0.3 tan θ	1.26 + 0.3 tan θ	1.00 + 0.3 tan θ	1.16 + 0.3 tan θ	0.95 + 0.3tan θ	0.3*
2θ range (deg)	5.84−40.00	6.18−50.00	5.20−49.99	5.08−50.00	5.38−50.00	3.94−50.00
no. of refls/unique refls	1627/1493	921/894	4853/4558	1648/1494	3338/3141	20574/7090
R_{int}	0.0437		0.0225		0.0177	0.0727
no. of obsvns	1134 ($I \geq 2\sigma(I)$)	808 ($I \geq 2\sigma(I)$)	3338 ($I \geq 2\sigma(I)$)	1149 ($I \geq 2\sigma(I)$)	2409 ($I \geq 2\sigma(I)$)	4043 ($I \geq 2\sigma(I)$)
no. of parameters	226	131	408	148	210	453
residals $R(F_o)$[b]/$Rw(F_o^2)$[a]	0.0318/0.0791	0.0300/0.0813	0.0397/0.1047	0.0340/0.0929	0.0320/0.0857	0.0916/0.3083
GOF	1.050	1.073	1.014	1.008	1.047	1.041
ΔQ in final ΔF map, e Å^{-3}	0.21 to −0.27	0.46 to −0.40	0.34 to −0.37	0.32 to −0.27	0.27 to −0.22	1.24 to −0.60
largest shift/esd, last cycle	0.00	0.00	0.03	0.00	0.00	0.00

[a] Radiation, Mo Kα, $\lambda = 0.710\ 73$ Å. [b] Conventional $R = R = \sum||F_o| - |F_c||/\sum|F_o|$ for observed reflections having $F_o^2 > 2\sigma(F_o^2)$. [c] $R_w = [\sum w(F_o^2 - F_c^2)^2/\sum w(F_o^2)^2]^{1/2}$ for all data.

(f) *r*-1-[(*Z*)-(4-Acetamidobenzylidene)amino-κN]-*c*-3,*c*-5-diamino-$\kappa^2 N,N'$-cyclohexanechlorozinc(II) tetraphenylborate·H_2O·CH_3OH (10). Zinc(II) chloride (0.012 g, 0.09 mmol) was dissolved in methanol (2 cm^3) and added to a solution of **4** (0.05 g, 0.09 mmol) in methanol (3 cm^3). A solution of sodium tetraphenylborate (0.03 g, 0.09 mmol) in methanol (1 cm^3) was added to the combined solution and left to stand for 4 days, after which colorless crystals formed. These were filtered off and dried *in vacuo* to afford the product as a white powder (0.03 g, 0.04 mmol, 44%). mp: 301−324 °C (dec). ^{1}H NMR (CD_3-OD, 270 MHz): δ 8.65 (s, 1H N=C*H*), 7.91 [m, 4H, Ar*H*], 4.95 (s, H_2O), 4.22 (m, 1H, CR_2H), 3.67 (m, 2H, CR_2H), 2.20 (s, 3H, $COCH_3$), 2.00 (m, 6H, $>CH_2$); *tetraphenylborate resonances*, δ 7.32 (m, 8H, Ar*H*), 7.00 (m, 8H, Ar*H*), 6.86 (m, 4H, Ar*H*). IR cm^{-1} (KBr pressed pellet): 3282 (s), 3244 (s), 3056 (m), 1680 (m), 1628 (s), 1603 (s), 1537 (s), 1516 (s), 1481 (m), 1428 (m), 1408 (m), 1322 (m), 1269 (m), 1183 (m), 1152 (m), 839 (m), 738 (s), 710 (s), 608 (m). MS LRFAB(NOBA matrix) +ve ion m/z = 373 (M^+, $-BPh_4^-$). Anal. Calcd for $C_{39}H_{42}N_4O$ B Cl Zn·CH_3OH·H_2O, actual (expected): C, 64.67 (64.53); H, 6.46 (6.50); N, 7.61 (7.53). Measured density: 1.25(5) g cm^{-3}.

X-ray Crystallographic Studies[18] of 5−10. Crystals of **5**−**10** were grown by slow evaporation of methanolic solutions of the complexes over a period of days. The resulting crystals of **5**−**9** were mounted on thin glass fibers with a coat of epoxy cement. X-ray data were collected on a Rigaku AFC6S diffractometer. Cell constants and an orientation matrix for the data collection were obtained from a least-squares refinement of the positions of 20 automatically centered reflections. Equivalent reflections were merged, and data were corrected for Lorentz and polarization factors. Absorption corrections were applied to the data collected for **5**−**7** and **9** on the basis of several azimuthal scans. Due to the solvent-sensitive nature of **10**, a crystal of **10** was mounted using the oil drop technique.[19] Data for **10** were collected at 160 K using a Siemens LT2 low-temperature system on a Siemens Smart CCD area detector diffractometer. Cell parameters were refined from the setting angles of 4924 reflections selected from the complete data set,[20] and reflections were measured to cover more than a hemisphere of data collected from frames each covering 0.3° in ω. A semiempirical absorption correction was applied with an ellipsoidal crystal shape model based on the high degree of data redundancy.

Table 2. Infrared Data (cm^{-1}) for the Ligands and Complexes

ligand	ν(N=C)	complex	ν(N=C)	ν(N−H)
1	1650 s	**5**	1619 s	3294 s, 3263 s
1		**6**	1637 s	3233 s, 3138 m
1		**7**	1634 s	3284 s, 3241 s
2	1644 s	**8**	1627 m	3220 s, 3136 s
3	1640 s	**9**	1629 m	3258 m, 3215 m
4	1639 s	**10**	1628 s	3282 s, 3244 s

Structures of **5**-**9** were solved using Patterson methods with SAPI91 and expanded using Fourier techniques with DIRDIF. Full-matrix least-squares refinement on F^2 was carried out with SHELXL 93. Programs used are given in ref 21. The structure of **10** was solved using the heavy-atom method and was refined by full-matrix least-squares on F^2 with SHELXTL. All non-hydrogen atoms were refined anisotropically. The hydrogen atoms were refined on all structures using a riding model with isotropic temperature factors 1.2 times that of their carrier atoms (1.5 times for methyl groups). Structure **10** contains a disordered methanol of crystallization which was refined to an occupancy of 70%. An isotropic extinction coefficient [x = 0.0009 (2)] was refined. Programs used are given in ref 22. Crystallographic details are summarized in Table 1 and selected bond lengths and angles are given in Tables 3−8, and ORTEP[23] representations are shown in Figures 1−6. Additional material available from the Cambridge Crystallographic Data

(18) We have published structures of **7**−**9** in preliminary communications: **7** in ref 12 and **8** and **9** in ref 13.
(19) Hope, H. *Acta Crystallogr.* **1988**, *B44*, 22.
(20) Clegg, W., University of Newcastle-upon-Tyne.
(21) Hai-Fu, F. SAPI91, structure analysis programs with intelligent control, Rigaku Corp., Tokyo, Japan, 1993. Beurskens, P. T.; Admiraal, G. Beurskens, G.; Bosman, G.; Garcia-Granda, W. P.; Gould, R. O.; Smits, J. M. M.; Smykalla, C; the DIRDIF program system, technical report of the crystallographic laboratory, University of Nijmegen, The Netherlands, 1992. Sheldrick, G. M. SHELXL 93, program for crystal structure refinement. University of Gottingen, Germany.
(22) Smart and Saint area detector control and integration software. Siemens Analytical X-ray Instruments Inc., Madison, WI. Sheldrick, G. M. SHELXTL Version 5 1994. Siemens Analytical X-ray Instruments Inc., Madison, WI.
(23) Johnson, C. K., ORTEP, Report ORNL-5138, Oak Ridge National Laboratory, Oak Ridge, TN, 1976.

Table 3. Selected Bond Lengths (Å) and Interbond Angles (deg) for **5**

Ni(1)−N(2)	2.021(4)	Ni(1)−O(2)	2.185(3)
Ni(1)−N(3)	2.057(4)	C(7)−C(8)	1.469(7)
Ni(1)−N(1)	2.076(4)	N(1)−C(7)	1.278(6)
Ni(1)−O(1)	2.124(3)	N(1)−C(4)	1.511(6)
Ni(1)−O(3)	2.155(3)		
N(2)−Ni(1)−N(3)	91.0(2)	N(3)−Ni(1)−O(3)	90.2(2)
N(2)−Ni(1)−N(1)	98.0(2)	N(1)−Ni(1)−O(3)	165.7(2)
N(3)−Ni(1)−N(1)	86.7(2)	O(1)−Ni(1)−O(3)	83.30(14)
N(2)−Ni(1)−O(1)	93.0(2)	N(2)−Ni(1)−O(2)	155.6(2)
N(3)−Ni(1)−O(1)	172.6(2)	N(3)−Ni(1)−O(2)	88.36(14)
N(1)−Ni(1)−O(1)	98.8(2)	N(1)−Ni(1)−O(2)	106.3(2)
N(2)−Ni(1)−O(3)	96.0(2)	O(1)−Ni(1)−O(2)	85.45(13)
N(1)−C(7)−C(8)	129.9(5)	O(3)−Ni(1)−O(2)	59.57(13)
C(9)−C(8)−C(7)	117.2(5)	C(7)−N(1)−C(4)	113.1(4)
C(13)−C(8)−C(7)	124.7(5)	C(7)−N(1)−Ni(1)	133.3(3)

Table 4. Selected Bond Lengths (Å) and Interbond Angles (deg) for **6**

Cu(1)−O(1)*1	1.968(3)	O(2)−C(1)	1.238(6)
Cu(1)−O(1)	1.968(3)	N(1)−C(7)	1.262(9)
Cu(1)−N(2)*1	2.006(4)	C(7)−C(8)	1.482(12)
Cu(1)−N(2)	2.006(4)	C(8)−C(13)	1.359(13)
Cu(1)−N(1)	2.401(7)	C(8)−C(9)	1.387(9)
O(1)−C(1)	1.272(5)	N(1)−C(6)	1.484(8)
O(1)*1−Cu(1)−O(1)	83.3(2)	C(7)−N(1)−C(6)	113.2(6)
O(1)*1−Cu(1)−N(2)*1	90.04(13)	C(13)−C(8)−C(7)	125.1(8)
O(1)−Cu(1)−N(2)*1	164.4(3)	C(9)−C(8)−C(7)	115.1(9)
O(1)*1−Cu(1)−N(2)	164.4(3)	C(7)−N(1)−Cu(1)	138.3(4)
O(1)−Cu(1)−N(2)	90.04(13)	C(6)−N(1)−Cu(1)	108.5(4)
N(2)*1−Cu(1)−N(2)	92.8(2)	N(1)−C(7)−C(8)	127.2(6)
O(1)*1−Cu(1)−N(1)	107.4(2)	C(1)−O(1)−Cu(1)	129.0(3)
O(1)−Cu(1)−N(1)	107.4(2)	O(2)−C(1)−O(1)	125.0(4)
N(2)*1−Cu(1)−N(1)	88.0(2)	O(2)−C(1)−C(2)	119.7(4)
N(2)−Cu(1)−N(1)	88.0(2)	O(1)−C(1)−C(2)	115.3(4)

Table 5. Selected Bond Lengths (Å) and Interbond Angles (deg) for **7**

Zn(1)−N(1)	2.035(3)	N(1)−C(7)	1.277(5)
Zn(1)−N(2)	2.026(3)	N(1)−C(1)	1.497(5)
Zn(1)−N(3)	2.045(3)	C(7)−C(8)	1.456(6)
Zn(1)−Cl(1)	2.195(2)		
N(2)−Zn(1)−N(1)	97.72(13)	N(1)−C(7)−C(8)	126.8(4)
N(2)−Zn(1)−N(3)	94.97(13)	C(13)−C(8)−C(7)	122.1(4)
N(1)−Zn(1)−N(3)	95.72(13)	C(9)−C(8)−C(7)	119.5(5)
N(2)−Zn(1)−Cl(1)	115.20(9)	C(10)−C(9)−C(8)	120.5(5)
N(1)−Zn(1)−Cl(1)	132.68(10)	C(11)−C(10)−C(9)	120.5(5)
N(3)−Zn(1)−Cl(1)	113.12(10)	C(10)−C(11)−C(12)	120.1(5)
C(7)−N(1)−C(1)	116.5(3)	C(13)−C(12)−C(11)	119.5(5)
C(7)−N(1)−Zn(1)	133.4(3)	C(8)−C(13)−C(12)	121.1(5)
C(1)-N(1)-Zn(1)	109.8(2)		

Centre comprises thermal parameters, positional coordinates, and bond lengths and angles.

Table 6. Selected Bond Lengths (Å) and Interbond Angles (deg) for **8**

Cu(1)−O(2)	1.980(2)	O(3)−C(12)	1.232(4)
Cu(1)−O(2)*1	1.980(2)	O(4)−C(10)	1.362(6)
Cu(1)−N(2)*1	1.990(3)	N(5)−C(5)	1.283(6)
Cu(1)−N(2)	1.990(3)	C(6)−C(5)	1.470(6)
Cu(1)−N(1)	2.395(4)	N(1)−C(1)	1.475(6)
O(2)−C(12)	1.278(4)		
O(2)−Cu(1)−O(2)*1	81.8(2)	O(3)−C(12)−O(2)	125.2(3)
O(2)−Cu(1)−N(2)*1	163.46(10)	O(3)−C(12)−C(13)	119.8(4)
O(2)*1−Cu(1)−N(2)*1	89.99(12)	O(2)−C(12)−C(13)	115.0(3)
O(2)−Cu(1)−N(2)	89.99(12)	C(7)−C(6)−C(11)	118.9(5)
O(2)*1−Cu(1)−N(2)	163.46(10)	C(7)−C(6)−C(5)	123.1(4)
N(2)*1−Cu(1)−N(2)	94.2(2)	C(11)−C(6)−C(5)	118.0(4)
O(2)−Cu(1)−N(1)	107.43(9)	N(1)−C(5)−C(6)	127.1(4)
O(2)*1−Cu(1)−N(1)	107.43(9)	C(5)−N(1)−C(1)	114.8(4)
N(2)*1−Cu(1)−N(1)	88.68(10)	C(5)−N(1)−Cu(1)	138.3(3)
N(2)−Cu(1)−N(1)	88.68(10)	C(1)−N(1)−Cu(1)	106.9(3)
C(12)−O(2)−Cu(1)	126.8(2)		

Table 7. Selected Bond Lengths (Å) and Interbond Angles (deg) for **9**

Cu(1)−N(1)	2.446(3)	O(1)−C(12)	1.364(4)
Cu(1)−N(2)	2.000(3)	O(1)−C(14)	1.425(4)
Cu(1)−N(3)	2.013(3)	O(2)−C(10)	1.365(4)
Cu(1)−Cl(2)	2.310(2)	O(2)−C(15)	1.424(4)
Cu(1)−Cl(1)	2.3121(14)	C(7)−C(8)	1.474(4)
N(1)−C(7)	1.274(4)	N(1)−C(1)	1.492(4)
N(2)−Cu(1)−N(3)	90.21(11)	N(3)−Cu(1)−N(1)	87.80(10)
N(2)−Cu(1)−Cl(2)	166.45(8)	Cl(2)−Cu(1)−N(1)	105.71(8)
N(3)−Cu(1)−Cl(2)	85.95(9)	Cl(1)−Cu(1)−N(1)	107.01(7)
N(2)−Cu(1)−Cl(1)	85.31(9)	N(1)−C(7)−C(8)	128.4(3)
N(3)−Cu(1)−Cl(1)	164.24(8)	C(12)−O(1)−C(14)	118.2(3)
Cl(2)−Cu(1)−Cl(1)	94.90(6)	C(10)−O(2)−C(15)	118.3(3)
N(2)−Cu(1)−N(1)	87.10(11)	C(9)−C(8)−C(7)	123.7(3)
		C(13)−C(8)−C(7)	115.7(3)

Table 8. Selected Bond Lengths (Å) and Interbond Angles (deg) for **10**

Zn(1)−N(1)	2.064(6)	C(7)−C(8)	1.439(13)
Zn(1)−N(2)	2.032(7)	C(11)−N(4)	1.354(13)
Zn(1)−N(3)	2.022(6)	N(4)−C(14)	1.21(2)
Zn(1)−Cl(1)	2.172(3)	C(14)−O(1)	1.37(2)
N(1)−C(7)	1.265(11)	C(14)−C(15)	1.57(2)
N(1)−C(1)	1.505(10)		
N(3)−Zn(1)−N(2)	96.9(3)	N(1)−C(7)−C(8)	125.8(8)
N(3)−Zn(1)−N(1)	93.2(2)	C(9)−C(8)−C(13)	117.7(10)
N(2)−Zn(1)−N(1)	95.3(3)	C(9)−C(8)−C(7)	117.8(9)
N(3)−Zn(1)−Cl(1)	111.8(2)	C(13)−C(8)−C(7)	124.4(10)
N(2)−Zn(1)−Cl(1)	118.2(2)	N(4)−C(11)−C(10)	120.1(13)
N(1)−Zn(1)−Cl(1)	133.7(2)	N(4)−C(11)−C(12)	122.2(13)
C(7)−N(1)−C(1)	116.6(7)	C(14)−N(4)−C(11)	134(2)
C(7)−N(1)−Zn(1)	132.7(6)	N(4)−C(14)−O(1)	124(2)
C(1)−N(1)−Zn(1)	110.3(5)	N(4)−C(14)−C(15)	123(2)
C(3)−N(2)−Zn(1)	110.7(5)	O(1)−C(14)−C(15)	113(2)
C(5)−N(3)−Zn(1)	112.3(4)		

Results and Discussion

The four ligands were synthesized by condensing tach with aldehydes to produce a series of triimine ligands (Scheme 1). The *E* isomer was exclusively produced, and the yield of the triimine ligand was >60%. In all cases, the complexation step with a transition metal caused the hydrolysis of two of the three imine groups, selectively producing an imine diamine complex (Scheme 2).[12,13] We presume that the main factor causing hydrolysis was due to destabilizing steric effects in an intermediate complex of the metal with the triimine.[24] CPK models indicate significant crowding in the triimine complex.

This selective complexation reaction is quite general and has been accomplished with nickel(II), copper(II), and zinc(II) salts and a variety of ligand derivatives. We present four ligands here, but the methodology may be extended to other aromatic aldehyde derivatives. The successful complexation producing the imine diamine complexes can been confirmed by IR. Comparison of the precursor ligand IR spectrum with that of the resulting complex shows that (see Table 2), on complexation, two new bands appear due to $\nu(NH_2)$. Also, the imine band, $\nu(C{=}N)$ moves to lower wavenumber (by $\sim$17 cm^{-1} on average), which is consistent with the weakening of the imine bond as a result of coordination to the metal. In the case of the zinc(II) complexes, the complexation can also be confirmed by ^1H NMR, with the imine proton shifting downfield in the complex with respect to the free ligand (on complexation the imine proton of **1** shifts from δ 8.38 to 8.85 and **4** from δ 8.43 to 8.65 ppm). The FAB^+ mass spectra show a parent peak,

(24) Brand, U.; Varhenkamp, H. *Inorg. Chim. Acta* **1992**, *198*−*200*, 663.

Scheme 1. Reaction of Tach with the Aldehydes to give Ligands **1**−**4**

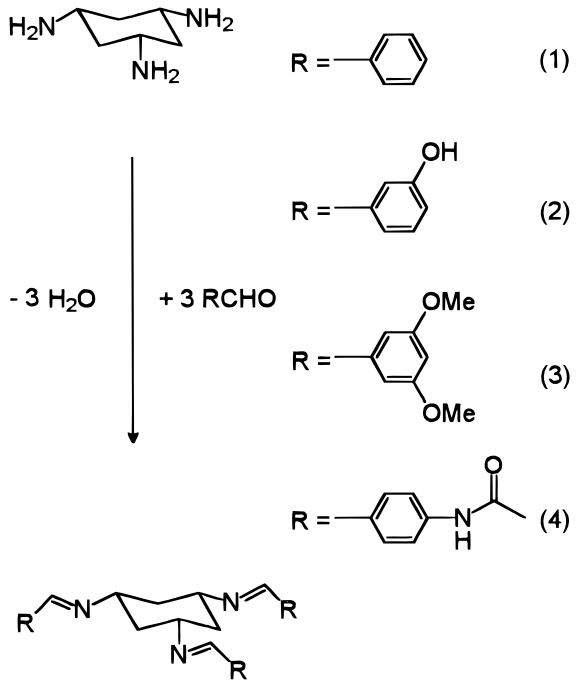

Scheme 2. Complexation of Ligands **1**−**4** To Give Complexes **5**−**10**[a]

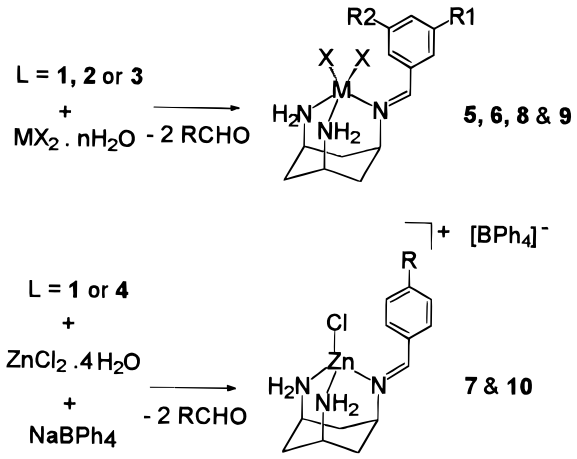

[a] **5**: M = Ni, X = NO_3, R1 = R2 = H. **6**: M = Cu, X = OAc, R1 = R2 = H. **7**: M = Zn, X = Cl, R = H. **8**: M = Cu, X = OAc, R1 = OH, R2 = H. **9**: M = Cu, X = Cl, R1 = R2 = OMe. **10**: M = Zn, X = Cl, R = $NHCOCH_3$.

which is due to the complex losing one anion [in the case of the copper complexes, peaks are also seen from the loss of the second anion and subsequent reduction of the copper (II) to copper (I)].

Compound 5. The structure of **5** is depicted in Figure 1. The tach moiety coordinates to the nickel center in a face-capping fashion. The remainder of the nickel's coordination sphere is taken up by one monodentate anion and one bidentate nitrate anion. There is a close phenyl hydrogen−oxygen contact between H(13) of the aromatic ring and O(1) of the monodentate nitrate anion [O(1)···H(13)−C(13), 168.4 (2)°; C(13)···O(1), 3.165 (6) Å]. The H···O distance of 2.249 (6) Å is 0.25 Å less than the sum of H and O van der Waals radii, consistent with a hydrogen bond interaction.[25] Steric interaction between the benzyl group and the nitrate anion significantly distorts the

(25) Thevent, G.; Rodier, N. *Bull. Chim. Soc. Fr.* **1981**, *11*−*12*, 437.

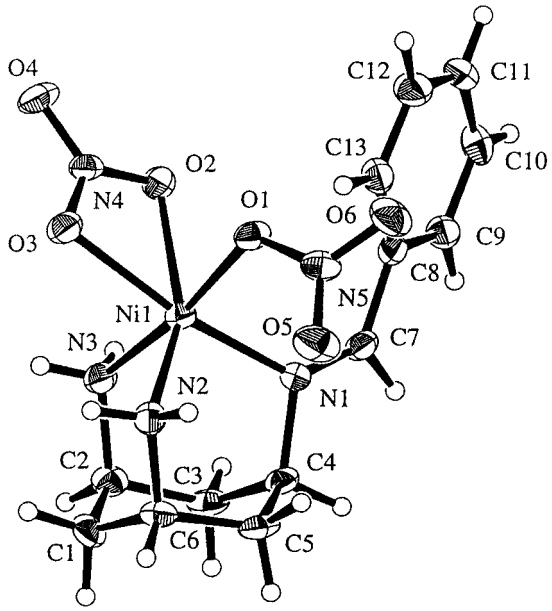

Figure 1. ORTEP[23] representation (30% probability thermal ellipsoids) of **5**.

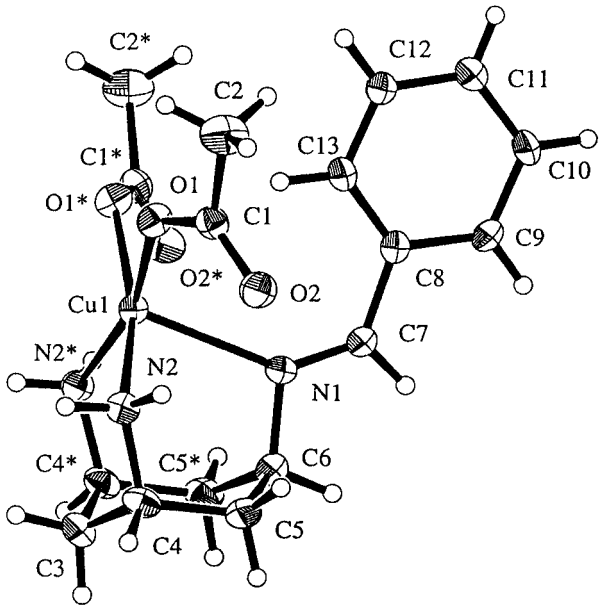

Figure 2. ORTEP[23] representation (30% probability thermal ellipsoids) of **6**.

benzyl geometry. The angles at Ni−N(1)−C(7) of 133.3(3)° and N(1)−C(7)−C(8) of 129.9 (5)° show that the benzyl is "bent back" from the nitrate anions. A torsion angle of 23.3 (9)° for [N(1)−C(7)−C(8)−C(9)] is further evidence of significant steric strain. Clearly, the benzyl group in **1** affects substrate coordination by creating an unsymmetrical, sterically congested coordination environment. This congestion is highlighted if the crystal structure of **5** is contrasted to that of Ni(tach)$(H_2O)_3$-$(NO_3)_2$.[26] This shows the tach and three water molecules completing the nickel coordination sphere with the nitrates as spectator counterions. In **5**, solvent does not coordinate to the metal ion, presumably due to unfavorable steric interactions with the benzyl group. Instead, less sterically demanding nitrate anions complete the coordination sphere.

Copper Compounds: 6, 8, and 9. The structures of **6**, **8**, and **9**[18] (Figures 2, 4 and 5) all show a five-coordinate copper

(26) Schwarzenbach, G.; Burgi, H.-B.; Jensen, W. P.; Lawrance, G. A.; Monsted, L.; Sargenson, A. M. *Inorg. Chem.* **1983**, *22*, 4029.

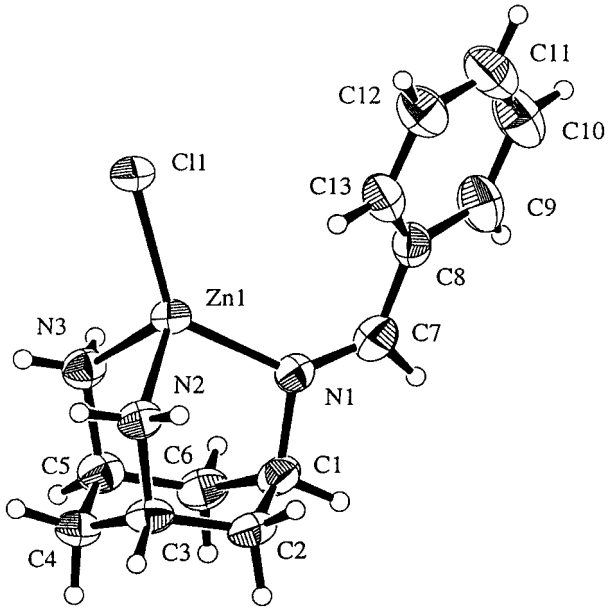

Figure 3. ORTEP[23] representation (30% probability thermal ellipsoids) of **7**. The tetraphenylborate anion and the methanol solvent molecule are omitted for clarity.

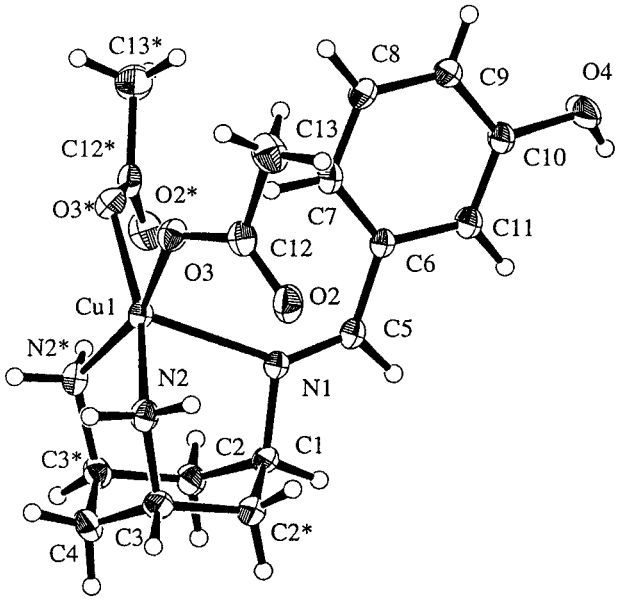

Figure 4. ORTEP[23] representation (30% probability thermal ellipsoids) of **8**.

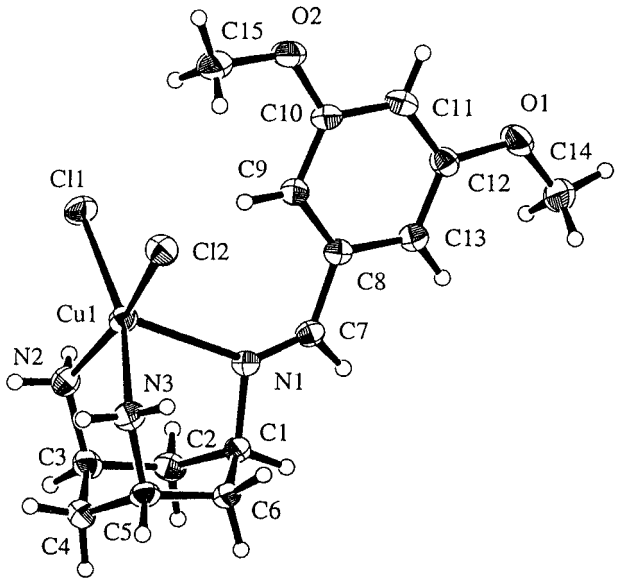

Figure 5. ORTEP[23] representation (30% probability thermal ellipsoids) of **9**.

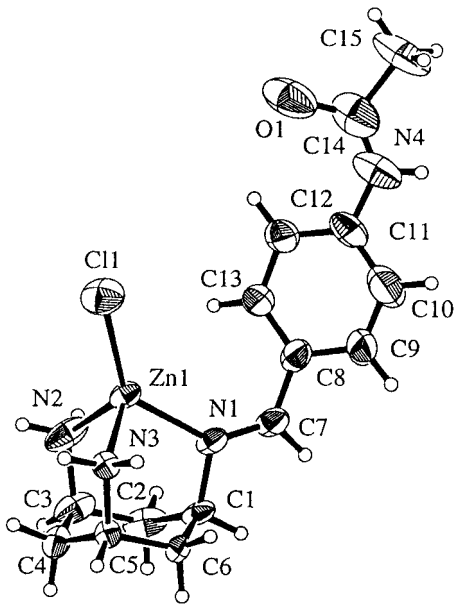

Figure 6. ORTEP[23] representation (30% probability thermal ellipsoids) of **10**. The tetraphenylborate anion the solvent molecules are omitted for clarity.

center ligated by two anions and by three face-capping nitrogens of the tach ligand. In each case, the copper coordination geometry is square pyramidal distorted along the apical Cu(1)−N(1) bond with a distance of 2.401(7) Å in **6**, 2.395(4) Å in **8**, and 2.446(3) Å in **9**. In **6** and **8** the phenyl ring and the imine form a perfectly planar unit (**6** and **8** lie on a crystallographic mirror plane); **9** forms a near-planar unit with a torsion angle of 2.9(5)° [N(1)−C(7)−C(8)−C(9)]. The N(1)−C(7)−C(8) angle is 128.4(3)° in **6**; the equivalent angle in **8** N(1)−C(5)−C(6) is 127.1(4)° and 128.4(3)° for N(1)−C(7)−C(8) in **9**, indicating some steric strain between the phenyl ring and the anions coordinated to the copper centre.

Zinc Compounds: 7 and 10. In **7** and **10** (Figures 3 and 6) the tach moiety is coordinated in a face-capping fashion, with the fourth coordination site on zinc occupied by a chloride anion. Steric interaction between the benzyl arm and the chloride anion significantly distorts the zinc coordination geometry and the benzyl geometry in each case. The angles at Zn(1)−N(1)−C(7) are 133.4(3) and 132.7(6)° for **7**[18] and **10**, respectively. The N(1)−C(7)−C(8) angles of 126.8(4)° and 125.8(8)° for **7** and **10**, respectively, show that the benzyl arm is "bent back" from the chloride anion. The torsion angles of 28.3(7)° for **7** and 25.9(2)° for **10** between [N(1)−C(7)−C(8)−C(13)] are evidence of steric strain, showing that the phenyl ring and the imine bond are non-planar. The zinc coordination geometry is distorted with a large Cl−Zn−N(1) angle of 133.7(2) and 133.7(1) in both **7** and **10**, respectively. In the copper complexes, the axial Cu−N(imine) bonds are elongated and thus can reduce the amount of steric interaction between the benzyl group and the anions coordinated to the metal. Like the copper complexes, both zinc complexes are isostructural except for differing substitution on the phenyl ring. In **10**, the acetamido moiety hydrogen bonds with a methanol molecule via the amide oxygen and to a water molecule via the amide nitrogen. The amide oxygen is placed 6.853(9) Å from the zinc ion.

Conclusions

Using the versatile tach ligand, we have shown that it is possible to prepare a range of benzylimine diamine complexes with different metal salts. The reaction scheme is general and gives the products in good yields. The complexes are essentially isostructural around the metal but differ in the substitution of the benzyl ring. As such, these complexes are systematically varied in the metal's secondary coordination environment. Future work will concentrate on improving the water solubility of these complexes, with a view to using them as bioinorganic model complexes.

Acknowledgment. We thank Prof. W. Clegg (University of Newcastle-upon-Tyne) for the use of the diffractometer and associated computer programs and equipment. L.C. and B.G. thank the EPSRC for the provision of maintenance grants.

Supporting Information Available: Full details of the crystal data including fractional coordinates, anisotropic displacement parameters, and full tables of bond lengths and angles for **5**−**10** (57 pages). Ordering information is given on any current masthead page.

IC9614529